ACS Photonics

Article

Cite This: ACS Photonics 2018, 5, 4056−4060

pubs.acs.org/journal/apchd5

Broadband Electrically Tunable Dielectric Resonators Using Metal−Insulator Transitions

Nikita A. Butakov,[†] Mark W. Knight,[‡] Tomer Lewi,[†] Prasad P. Iyer,[†] David Higgs,[†] Hamid T. Chorsi,[†] Juan Trastoy,[§] Javier Del Valle Granda,[§] Ilya Valmianski,[§] Christian Urban,[§] Yoav Kalcheim,[§] Paul Y. Wang,[§] Philip W. C. Hon,[‡] Ivan K. Schuller,[§] and Jon A. Schuller*,[†]

[†]Department of Electrical & Computer Engineering, University of California, Santa Barbara, Santa Barbara, California 93106, United States

[‡]NG Next Northrop Grumman Corporation, 1 Space Park Drive, Redondo Beach, California 90278, United States

[§]Department of Physics, University of California, San Diego, La Jolla, California 92093, United States

Supporting Information

ABSTRACT: Dielectric-resonator-based nanophotonic devices show promise owing to their low intrinsic losses, support of multipolar resonances, and efficient operation in both reflection and transmission configurations. A key challenge is to make such devices dynamically switchable, such that optical behavior can be instantaneously reconfigured. In this work we experimentally demonstrate large, broadband, and continuous electrical tuning of reflection resonances in hybrid dielectric−VO_2 devices. Our calculations, in strong agreement with experimental reflectance measurements, also indicate the presence of large transmission and absorption modulation. We additionally demonstrate independent modulation of both reflection amplitude and phase at Fabry−Pérot anti-nodes and nodes, respectively, a key requirement for metasurface design. We conclude with a temporal characterization, in which we achieve rapid electronic modulation rates of approximately 3 kHz, substantially faster than other recent approaches. These findings greatly expand the potential of designing nanophotonic devices that exploit the tunable behavior of hybrid dielectric−VO_2 resonators.

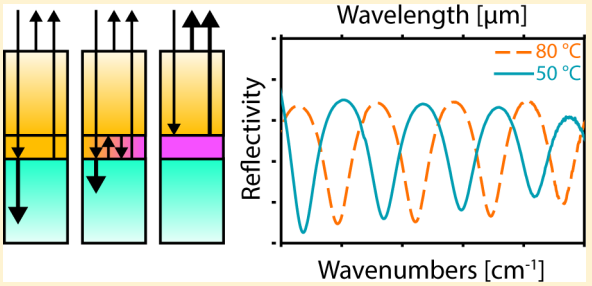

KEYWORDS: *vanadium dioxide, metasurface, metamaterial, reconfigurable, metal−insulator transition, active nanophotonics*

Vanadium dioxide (VO_2), since the discovery of its metal−insulator phase transition behavior,[1,2] has been a keen subject of study for applications in reconfigurable electronic,[3,4] mechanical,[5,6] thermal,[7,8] and optical systems. Early demonstrations of thermally switchable gratings[9] and zone plates[10] showcased the potential of VO_2-based reconfigurable nanooptics. For switchable metamaterials, various plasmonic systems (e.g., split-ring resonators) have been integrated onto thin films of VO_2.[11−13] Alternative switching approaches include ion-gel gating,[14] defect engineering,[15] and terahertz pump−probe[16] techniques. Early examples of electronically triggered devices demonstrated nanosecond switching rates in ultracompact waveguide electroabsorption modulators.[17,18] More recently, large-area plasmonic metamaterial-based modulators have exhibited important advances in reducing switching energies[19] and demonstrating optical memory behavior.[20] Despite numerous recent explorations of low-loss, high-efficiency dielectric free-space optics,[21,22] examples of hybrid dielectric−VO_2 reconfigurable optics are lacking.

In this work, we show that hybrid dielectric−VO_2 structures display several novel behaviors of great interest in the development of reconfigurable optics. These include independent tuning of the reflection amplitude and phase, large modulation of transmission and absorption, and kHz-scale electronic switching rates. The active surface proposed in this work uses VO_2, in which there is a large change in infrared reflectivity across a temperature-driven metal−insulator phase transition (MIT). We show that the effects of the MIT can be enhanced by adding overlying resonant structures, the simplest of which is a Fabry−Pérot (FP) cavity. With such a structure we demonstrate continuous tuning of the reflection, transmission, and absorption resonances across the MIT. With proper design, switching the VO_2 film causes the reflectance spectrum to invert. Using a custom-built mid-infrared Michaelson interferometer system, we find that at the anti-nodes, where reflection minima transform into reflection maxima, the phase remains constant across the MIT. At the nodes, however, where the reflection is the same in both the insulating and metallic states, the amplitude remains constant, while the phase exhibits a continuous shift. Finally, we conclude by triggering the MIT with brief (60 μs) electronic pulses and demonstrating switching rates of approximately 3 kHz.

Received: May 23, 2018
Published: September 9, 2018

DOI: 10.1021/acsphotonics.8b00699
ACS Photonics 2018, 5, 4056−4060

THERMALLY TUNABLE FABRY–PÉROT CAVITY

In correlated materials, electron–electron interactions lead to exotic emergent properties such as metal–insulator phase transitions. Across this transition, the optical constants undergo a dramatic shift,[23] which is of great interest in the design of reconfigurable optical devices. At the interface between a transparent material and VO_2, as expected of a transition between metallic and insulating optical properties, the reflectivity undergoes a π phase shift across the MIT. Here, MIT reflection-phase switching modulates the complex reflectivity (i.e., amplitude and phase), transmission, and absorption of a simple Ge–VO_2 tunable Fabry–Pérot (TFP) resonator (Figure 1a). Ge, in particular, is used due its

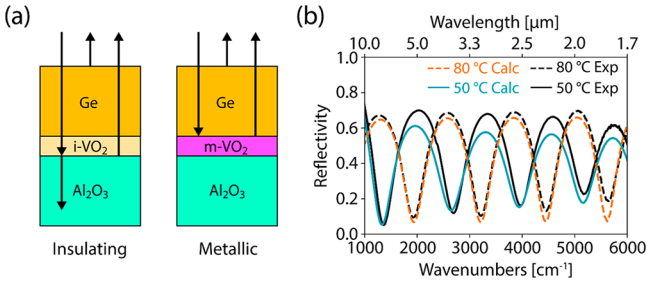

Figure 1. Temperature-Tunable Fabry–Pérot cavity. (a) Schematic of Ge–VO_2–Al_2O_3 device in the insulating and metallic states. The arrows represent the dominant reflection interfaces. (b) Line plot of the analytically calculated and experimentally measured reflectivity, of a 1 μm thick Ge Fabry–Pérot cavity, on a 100 nm thick film of VO_2, on an R-cut sapphire substrate. Simulation, sample fabrication, optical constants, and measurement details are included in the Supporting Information.

relatively high refractive index ($n \approx 4$) and favorable electronic conductivity. When the underlying VO_2 film is in its insulating phase (solid black line), the cavity exhibits a broadband low-loss IR FP spectrum (Figure 1b). When the VO_2 is switched to the metallic phase (dashed black line), the spectrum inverts, due to the additional π reflection phase imposed at the Ge–VO_2 interface. The Supporting Information shows that this phase shift is smooth and continuous across the MIT. Local reflection maxima become minima and vice versa, providing large-magnitude (10%–70%) switching of reflection amplitudes spanning a 20-fold frequency range from the long-wave-infrared (20 μm) to near-infrared (1 μm, near-infrared spectra included in the Supporting Information). The focus, herein, is on the 1000–6000 cm^{-1} (1.7–10 μm) infrared frequency band. At lower and higher wavelengths FP resonance switching is observed but complicated by interaction with Al_2O_3 phonons and VO_2 absorption, respectively.

Our experimental measurements are in strong agreement with analytical calculations (blue and dashed orange lines), with only small deviations, which may be attributed to experimental imperfections (e.g., light-absorbing defects, unintentional doping). In our analytical investigations, included in the Supporting Information, we find that this inversion behavior is highly dependent upon the Ge and VO_2 thicknesses and optical constants, as well as the presence of a low-index substrate. In the insulating state, due to the similar refractive indices of the Ge and VO_2 layers (around 4 and 3, respectively), the effective thickness of the Fabry–Perot cavity is approximately the sum of the Ge and VO_2 layer thicknesses. This causes a small offset between the insulating phase minima and metallic phase maxima, which becomes substantial when the VO_2 thickness becomes comparable with the Ge layer. For example, if the VO_2 is 300 nm thick, reflection minima do not transform into reflection maxima at the same wavelength. At very low thicknesses, on the other hand, we find that the metallic state VO_2 does not reflect the majority of incident light. Therefore, balanced thicknesses, and likewise balanced refractive indices, are required to achieve the desired inversion behavior.

MODULATING THE REFLECTION AMPLITUDE AND PHASE

Unlike existing switchable VO_2 photonic devices, we further exploit the mesoscopic, continuous nature of the MIT in VO_2 thin films to achieve *continuous* reflection modulation, as well as independent control over the phase, a key requirement for the construction of high-efficiency metasurfaces. Using a custom-built mid-infrared Michaelson interferometer,[24] we experimentally measure the reflection phase and amplitude of a TFP and compare the results against calculations using the transfer-matrix method (Figure 2). Experimentally measured

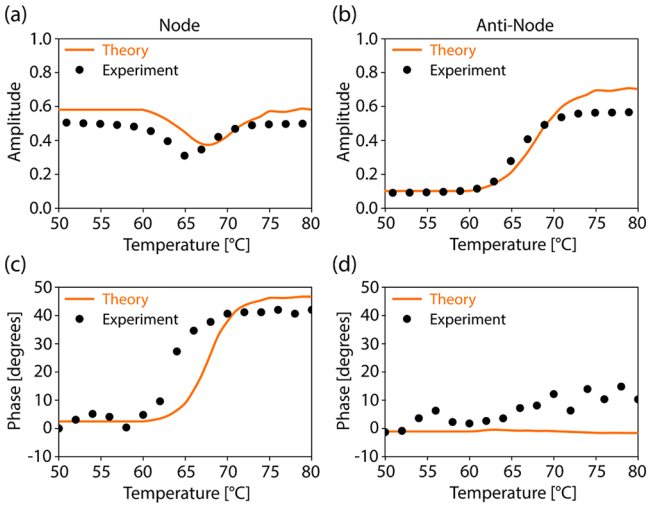

Figure 2. Amplitude and phase modulation. Reflection amplitude (a, b) and phase (c, d) at a TFP node (a, c) and anti-node (b, d). Here, the anti-node corresponds to 8 μm (1250 cm^{-1}) and the node corresponds to 10.5 μm (950 cm^{-1}). Experimental data are shown as black dots. Calculated predictions, based on fitted VO_2 optical constants, are shown as orange, solid lines.

reflectivities of the TFP *across* the MIT exhibit smooth, continuous variations. At TFP nodes, the points at which the fully insulating and fully metallic states intersect in Figure 1b, the reflection amplitude is unchanged between the extremes, with a suppression at intermediate temperatures due to increased absorption as VO_2 passes through the epsilon-near-zero regime[25−28] (Figure 2a). At the anti-nodes, on the other hand, there is a large, continuous amplitude shift as the TFP switches between fully insulating and fully metallic regimes (Figure 2b). With temperature control we achieve stable, repeatable, and continuous sampling of reflection amplitudes. Using previously derived VO_2 optical constants[29] (see Supporting Information) we see that this behavior largely originates from a continuous variation in reflection phase at the Ge–VO_2 interface (see Supporting Information). Calculated reflectance shows good agreement with experiment.

DOI: 10.1021/acsphotonics.8b00699
ACS Photonics 2018, 5, 4056–4060

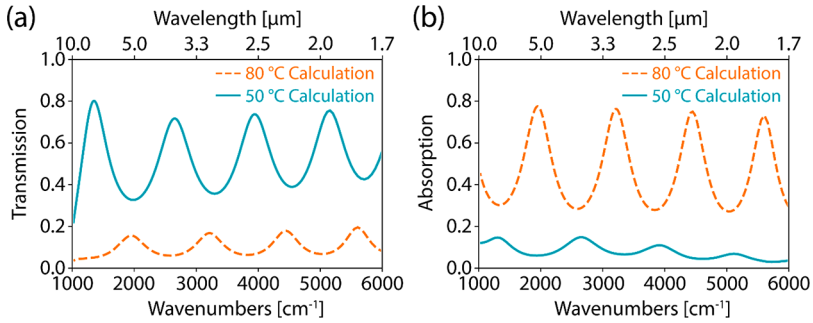

Figure 3. Temperature-tunable transmission and absorption. (a) Line plot of the analytically calculated transmission spectra of a 1 μm thick Ge Fabry–Pérot cavity on a 100 nm thick film of VO_2 and on an R-cut sapphire substrate. (b) Line plot of the corresponding analytically calculated absorption spectra.

In addition to modulating the amplitude of reflectance or absorption, TFPs are useful for phase modulation. At the TFP anti-node the large shift in amplitude (Figure 2b) is accompanied by an approximately constant phase (Figure 2d). At the TFP node, this behavior is interchanged. The amplitude undergoes a small drop at intermediate temperatures (Figure 2a) but is otherwise mostly constant. The phase (Figure 2c), on the other hand, undergoes a shift of approximately 0.7 radians (40 degrees). The observed phase shifts could, potentially, be further enhanced through more sophisticated distributed-Bragg-reflector design or by patterning the Ge layer to form Mie resonators.[30,31] In either case, TFP anti-nodes are most useful for amplitude modulation, and TFP nodes for phase modulation.

TUNABLE TRANSMISSION AND ABSORPTION

Unlike other hybrid plasmonic–VO_2 metasurface structures,[12,19,20,32] which are limited to reflection mode operation due to metallic ground planes, this device architecture supports high transmission when in the low-temperature insulating phase (Figure 3a). The device can be used for large transmission modulation between $T \approx 0.05$ and $T \approx 0.8$ at TFP antinodes. Across the intermediate temperatures (included in the Supporting Information) there is a smooth and continuous variation in the transmission. Alternatively, the device can be used for large absorption modulation from $A \approx 0.1$ to $A \approx 0.8$ (Figure 3b). In the high-temperature metallic phase, the reflection minima (Figure 1b) coincide with absorption resonances, which arise from the relatively low conductivity of VO_2 in its metallic state. This behavior would not be apparent in high-conductivity metals such as Au or Ag. At those same wavelengths, absorption in the insulating state is nearly absent (<10%). Color plots with the intermediate temperatures, included in the Supporting Information, demonstrate how VO_2-based TFPs can serve as continuously tunable absorbers: the absorption can be smoothly varied between $A \approx 0.1$ and $A \approx 0.7$. Unlike other metal–dielectric hybrid absorbers, comprising absorbing semiconductor films on highly reflective low-loss metallic substrates,[33,34] this system relies on lossless dielectric resonators placed on a film with switchable reflection and absorption properties. Further improvements in either transmission or absorption contrast may be achieved either through more sophisticated design of the FP parameters, using a distributed Bragg reflector for example, or by increasing electromagnetic confinement through the use of dielectric Mie resonators.[35,36]

ELECTRICALLY TUNABLE DEVICES

For the design of reconfigurable metasurfaces, it is necessary to locally modulate optical properties. To achieve electrically controllable devices, we modulate the TFP through Joule heating by passing current directly through a 200 μm × 200 μm TFP (Figure 4b inset). In the VO_2 insulating state, current

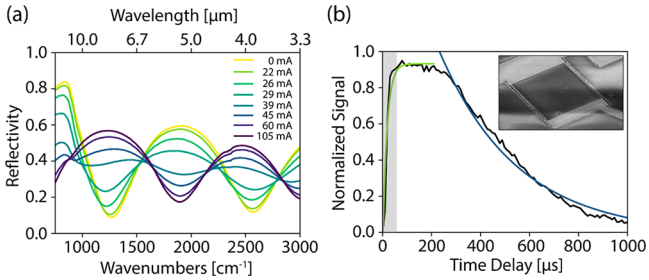

Figure 4. Electrically tunable Fabry–Pérot. (a) Experimentally measured FTIR reflectivity of a TFP, with Ge thickness 850 nm, as the applied DC current is varied. (b) Experimentally measured, normalized, transient reflectivity at the anti-node. The shaded region corresponds to the time over a which a 26 V, 60 μs square pulse is applied. The colored lines correspond to fitted exponential curves (orange, heating; blue, cooling). The inset shows an SEM of the corresponding device.

passes predominantly through the lightly doped Ge layer. This enables Joule heating of the device in both metallic and insulating VO_2 states, without requiring additional lossy metals. In Figure 4a we plot the reflectivity, as measured through an FTIR microscope, of an electrically controlled TFP as the DC source current is increased. The TFP is held at an ambient temperature of 57 °C, just below the MIT, to reduce the amount of power needed to induce the phase transition. The electrical TFP spectra are nearly identical to the thermal TFP spectra in Figure 1a, aside from differences arising from variations in the two film thicknesses. Similar to Figure 1, the TFP anti-nodes also exhibit continuous amplitude modulation. IR imaging of the device, as the current is increased (see video in Supporting Information), indicates that the MIT proceeds, for the most part, homogeneously across the 200 μm × 200 μm area. We attribute this behavior, as opposed to localized metallic filament formation, to the dual role the germanium layer plays in both carrying current and evenly redistributing heat (see Supporting Information).

The temporal dynamics are investigated by holding the device at 57 °C, applying a square voltage pulse (24 V, 60 μs), and monitoring the subsequent rise and decay of the anti-node

DOI: 10.1021/acsphotonics.8b00699
ACS Photonics 2018, 5, 4056–4060

reflectance using time-resolved FTIR spectroscopy (Figure 4b). To reduce the rise time, we use a voltage larger than the threshold value of 13 V (see Supporting Information for DC *IV* curves). We observe a fast rise, due to rapid Joule heating, followed by a slower, thermal-diffusion-limited decay. Dynamic traces exhibit an approximately 18 μs rise time, as determined through an exponential fit (see Supporting Information) with an approximately 315 μs decay time, corresponding to estimated modulation rates on the order of 3 kHz. When applying even larger voltages, faster rise times can be achieved (see Supporting Information). These values are 1 order of magnitude faster than the existing large-area VO_2 optical modulators,[19,20] which have rise times of >2.3 ms and relaxation times of <1.27 ms (corresponding to ∼280 Hz modulation rates). The decay time is likely limited by the relatively large thermal capacitance of the device and may be improved with metasurface structures that reduce the Ge and VO_2 volumes. Further improvements in speed can be attained by reducing the modulation depth or by instead utilizing a vertical contact geometry.[37] Further performance improvements can likely be achieved by optimizing the Ge layer's doping levels and the choice of metallic contacts for improved ohmic contacts.

We have used the metal−insulator phase transition of VO_2 to create electrically reconfigurable, continuously tunable nanophotonic devices operating across a broad infrared frequency range. By placing Ge resonators on a VO_2 thin film, we experimentally showed that infrared Fabry−Pérot reflection resonances can be continuously tuned by driving the underlying VO_2 film across the phase transition. Additionally, we experimentally demonstrated independent modulation of both reflection amplitude and phase at the Fabry−Perot nodes and anti-nodes. Our results, backed by strong agreement with analytical models, indicate that the hybrid device also exhibits strong transmission and absorption modulation. Electronically triggered reflectance measurements revealed switching rates on the order of 3 kHz. These findings expand the potential of engineering new nanophotonic devices and active metasurfaces, such as switchable gratings and zoom lenses,[38] that take advantage of the reconfigurable properties of hybrid semiconductor−VO_2 architectures.

■ ASSOCIATED CONTENT

Supporting Information

The Supporting Information is available free of charge on the ACS Publications website at DOI: 10.1021/acsphotonics.8b00699.

Detailed descriptions of methods and additional simulation and experimental data (PDF)

A Mathematica notebook containing transfer-matrix models of the Ge-VO_2 device, with analyses of alternative device geometries (ZIP)

A zip file containing the temperature-dependent mid-infrared optical permittivity of a 100 nm VO_2 film on an R-cut sapphire substrate (ZIP)

An IR video of a Ge-VO_2 device undergoing an electrically driven insulator−metal phase transition (ZIP)

■ AUTHOR INFORMATION

Corresponding Author

*E-mail: jonschuller@ece.ucsb.edu.

ORCID

Mark W. Knight: 0000-0001-7625-403X
Juan Trastoy: 0000-0002-5920-4302
Yoav Kalcheim: 0000-0002-1489-0505
Jon A. Schuller: 0000-0001-6949-3569

Author Contributions

This is highly collaborative research. The experiments were conceived jointly between all the authors. N.A.B. performed the calculations, numerical simulations, sample fabrication, and FTIR characterization. I.V., C.U., J.T.Q., J.D.V.G., and Y.K. grew the VO_2 thin films and performed transport measurements. T.L. performed the time-resolved FTIR step-scan measurements. P.I. and M.K. performed the infrared phase measurements. P.W. performed thermal simulations. H.C. performed infrared imaging measurements. D.H. assisted with numerical calculations and simulations. N.A.B. wrote the original draft of the manuscript, which then underwent multiple iterations between all the coauthors. P.H., J.A.S., and I.K.S. supervised the research project. We are grateful for discussions with Tanya Das, Steven Brown, and Ryan DeCrescent.

Notes

The authors declare no competing financial interest.

■ ACKNOWLEDGMENTS

This work was supported by the Air Force Office of Scientific Research (FA9550-16-1-0393 and FA9550-12-1-0381), by the UC Office of the President Multicampus Research Programs and Initiatives (MR-15-328528), and by a National Science Foundation CAREER award (DMR-1454260). Numerical calculations for this work were performed on the computing cluster at the Center for Scientific Computing from the California NanoSystems Institute at the University of California, Santa Barbara: an NSF MRSEC (DMR-1121053) and NSF CNS-0960316. We acknowledge support from the Vannevar Bush Faculty Fellowship program sponsored by the Basic Research Office of the Assistant Secretary of Defense for Research and Engineering and funded by the Office of Naval Research through grant N00014-15-1-2848. Thin films were prepared at the UCSD Nanoscience Center, and nanostructures were fabricated at the UCSB Nanofabrication Facility. This research was conducted with government support under the DoD, Air Force Office of Scientific Research, National Defense Science and Engineering Graduate (NDSEG) Fellowship, 32 CFR 168a. This work was also funded by NG Next, Northrop Grumman Corporation.

■ REFERENCES

(1) Morin, F. J. Oxides which show a metal-to-insulator transition at the Neel temperature. *Phys. Rev. Lett.* **1959**, *3*, 34.

(2) Barker, A. S.; Verleur, H. W.; Guggenheim, H. J. Infrared optical properties of vanadium dioxide above and below the transition temperature. *Phys. Rev. Lett.* **1966**, *17*, 1286.

(3) Kim, H.; Chae, B.; Youn, D.; Maeng, S.; Kim, G.; Kang, K. Mechanism and observation of Mott transition in VO_2-based two-and three-terminal devices. *New J. Phys.* **2004**, *6*, 52.

(4) Yang, Z.; Zhou, Y.; Ramanathan, S. Studies on room-temperature electric-field effect in ionic-liquid gated VO_2 three-terminal devices. *J. Appl. Phys.* **2012**, *111*, 014506.

(5) Liu, K.; Cheng, C.; Cheng, Z.; Wang, K.; Ramesh, R.; Wu, J. Giant-Amplitude, High-Work Density Microactuators with Phase Transition Activated Nanolayer Bimorphs. *Nano Lett.* **2012**, *12*, 6302−6308.

DOI: 10.1021/acsphotonics.8b00699
ACS Photonics 2018, 5, 4056−4060

(6) Rúa, A.; Fernández, F. E.; Sepúlveda, N. Bending in VO2-coated microcantilevers suitable for thermally activated actuators. *J. Appl. Phys.* **2010**, *107*, 074506.
(7) Ben-Abdallah, P.; Biehs, S. A. Near-field thermal transistor. *Phys. Rev. Lett.* **2014**, *112*, 044301.
(8) Wu, S.; Chen, M.; Barako, M. T.; Jankovic, V.; Hon, P. W. C.; Sweatlock, L. A.; Povinelli, M. L. Thermal homeostasis using microstructured phase-change materials. *Optica.* **2017**, *4*, 1390−1396.
(9) Zimmer, J.; Wixforth, A.; Karl, H.; Krenner, H. J. Ion beam synthesis of nanothermochromic diffraction gratings with giant switching contrast at telecom wavelengths. *Appl. Phys. Lett.* **2012**, *100*, 231911.
(10) Jostmeier, T.; Zimmer, J.; Karl, H.; Krenner, H. J.; Betz, M. Optically imprinted reconfigurable photonic elements in a VO_2 nanocomposite. *Appl. Phys. Lett.* **2014**, *105*, 071107.
(11) Dicken, M. J.; Aydin, K.; Pryce, I. M.; Sweatlock, L. A.; Boyd, E. M.; Walavalkar, S.; Ma, J.; Atwater, H. A. Frequency tunable near-infrared metamaterials based on VO_2 phase transition. *Opt. Express* **2009**, *17*, 18330−18339.
(12) Kocer, H.; Butun, S.; Banar, B.; Wang, K.; Tongay, S.; Wu, J.; Aydin, K. Thermal tuning of infrared resonant absorbers based on hybrid gold-VO_2 nanostructures. *Appl. Phys. Lett.* **2015**, *106*, 161104.
(13) Driscoll, T.; Palit, S.; Qazilbash, M. M.; Brehm, M.; Keilmann, F.; Chae, B.; Yun, S.; Kim, H.; Cho, S. Y.; Jokerst, N. M.; Smith, D. R.; Basov, D. N. Dynamic tuning of an infrared hybrid-metamaterial resonance using vanadium dioxide. *Appl. Phys. Lett.* **2008**, *93*, 024101.
(14) Goldflam, M.; Liu, M. K.; Chapler, B. C.; Stinson, H. T.; Sternbach, A. J.; McLeod, A. S.; Zhang, J. D.; Geng, K.; Royal, M.; Kim, B.; Averitt, R. D.; Jokerst, N. M.; Smith, D. R.; Kim, H.; Basov, D. T. Voltage switching of a VO_2 memory metasurface using ionic gel. *Appl. Phys. Lett.* **2014**, *105*, 041117.
(15) Rensberg, J.; Zhang, S.; Zhou, Y.; McLeod, A. S.; Schwarz, C.; Goldflam, M.; Liu, M.; Kerbusch, J.; Nawrodt, R.; Ramanathan, S.; Basov, D. N.; Capasso, F.; Ronning, C.; Kats, M. A. Active Optical Metasurfaces Based on Defect-Engineered Phase-Transition Materials. *Nano Lett.* **2016**, *16*, 1050−1055.
(16) Liu, M.; Hwang, H. Y.; Tao, H.; Strikwerda, A. C.; Fan, K.; Keiser, G. R.; Sternbach, A. J.; West, K. G.; Kittiwatanakul, S.; Lu, J.; Wolf, S. A.; Omenetto, F. G.; Zhang, X.; Nelson, K. A.; Averitt, R. D. Terahertz-field-induced insulator-to-metal transition in vanadium dioxide metamaterial. *Nature* **2012**, *487*, 345.
(17) Joushaghani, A.; Jeong, J.; Paradis, S.; Alain, D.; Aitchison, J. S.; Poon, J. K. S. Wavelength-size hybrid Si-VO_2 waveguide electroabsorption optical switches and photodetectors. *Opt. Express* **2015**, *23*, 3657−3668.
(18) Markov, P.; Marvel, R. E.; Conley, H. J.; Miller, K. J.; Haglund, R. F.; Weiss, S. M. Optically monitored electrical switching in VO_2. *ACS Photonics* **2015**, *2*, 1175−1182.
(19) Zhu, Z.; Evans, P. G.; Haglund, R. F.; Valentine, J. G. Dynamically reconfigurable metadevice employing nanostructured phase-change materials. *Nano Lett.* **2017**, *17*, 4881−4885.
(20) Liu, L.; Kang, L.; Mayer, T. S.; Werner, D. H. Hybrid metamaterials for electrically triggered multifunctional control. *Nat. Commun.* **2016**, *7*, 13236.
(21) Das, T.; Iyer, P. P.; DeCrescent, R. A.; Schuller, J. A. Beam engineering for selective and enhanced coupling to multipolar resonances. *Phys. Rev. B: Condens. Matter Mater. Phys.* **2015**, *92*, 241110.
(22) Arbabi, A.; Horie, Y.; Bagheri, M.; Faraon, A. Dielectric metasurfaces for complete control of phase and polarization with subwavelength spatial resolution and high transmission. *Nat. Nanotechnol.* **2015**, *10*, 937−943.
(23) Qazilbash, M. M.; Brehm, M.; Chae, B.; Ho, P.; Andreev, G. O.; Kim, B.; Yun, S. J.; Balatsky, A. V.; Maple, M. B.; Keilmann, F.; Kim, H.; Basov, D. N. Mott transition in VO_2 revealed by infrared spectroscopy and nano-imaging. *Science* **2007**, *318*, 1750−1753.
(24) Sherrott, M. C.; Hon, P. W. C.; Fountaine, K. T.; Garcia, J. C.; Ponti, S. M.; Brar, V. W.; Sweatlock, L. A.; Atwater, H. A. Experimental demonstration of > 230° phase modulation in gate-tunable graphene−gold reconfigurable mid-infrared metasurfaces. *Nano Lett.* **2017**, *17*, 3027−3034.
(25) Butakov, N. A.; Schuller, J. A. Hybrid optical antennas with photonic resistors. *Opt. Express* **2015**, *23*, 29698−29707.
(26) Park, J.; Kang, J.; Liu, X.; Brongersma, M. L. Electrically tunable epsilon-near-zero (ENZ) metafilm absorbers. *Sci. Rep.* **2015**, *5*, 15754.
(27) Huang, Y.; Howard Lee, H. W.; Sokhoyan, R.; Pala, R. A.; Thyagarajan, K.; Han, S.; Tsai, D. P.; Atwater, H. A. Gate-tunable conducting oxide metasurfaces. *Nano Lett.* **2016**, *16*, 5319−5325.
(28) Iyer, P. P.; Pendharkar, M.; Palmstrøm, C. J.; Schuller, J. A. Ultrawide thermal free-carrier tuning of dielectric antennas coupled to epsilon-near-zero substrates. *Nat. Commun.* **2017**, *8*, 472.
(29) Butakov, N. A.; Valmianski, I.; Lewi, T.; Urban, C.; Ren, Z.; Mikhailovsky, A. A.; Wilson, S. D.; Schuller, I. K.; Schuller, J. A. Switchable Plasmonic−Dielectric Resonators with Metal−Insulator Transitions. *ACS Photonics* **2018**, *5*, 371−377.
(30) Butakov, N. A.; Schuller, J. A. Designing multipolar resonances in dielectric metamaterials. *Sci. Rep.* **2016**, *6*, 38487.
(31) Lewi, T.; Evans, H. A.; Butakov, N. A.; Schuller, J. A. Ultrawide Thermo-optic Tuning of PbTe Meta-Atoms. *Nano Lett.* **2017**, *17*, 3940−3945.
(32) Kocer, H.; Butun, S.; Palacios, E.; Liu, Z.; Tongay, S.; Fu, D.; Wang, K.; Wu, J.; Aydin, K. Intensity tunable infrared broadband absorbers based on VO_2 phase transition using planar layered thin films. *Sci. Rep.* **2015**, *5*, 13384.
(33) Kim, S. J.; Park, J.; Esfandyarpour, M.; Pecora, E. F.; Kik, P. G.; Brongersma, M. L. Superabsorbing, artificial metal films constructed from semiconductor nanoantennas. *Nano Lett.* **2016**, *16*, 3801−3808.
(34) Kats, M. A.; Blanchard, R.; Genevet, P.; Capasso, F. Nanometre optical coatings based on strong interference effects in highly absorbing media. *Nat. Mater.* **2013**, *12*, 20.
(35) Lewi, T.; Iyer, P. P.; Butakov, N. A.; Mikhailovsky, A. A.; Schuller, J. A. Widely Tunable Infrared Antennas Using Free Carrier Refraction. *Nano Lett.* **2015**, *15*, 8188−8193.
(36) Iyer, P. P.; Butakov, N. A.; Schuller, J. A. Reconfigurable semiconductor phased-array metasurfaces. *ACS Photonics* **2015**, *2*, 1077−1084.
(37) Iyer, P. P.; Pendharkar, M.; Schuller, J. A. Electrically reconfigurable metasurfaces using heterojunction resonators. *Adv. Opt. Mater.* **2016**, *4*, 1582−1588.
(38) Yin, X.; Steinle, T.; Huang, L.; Taubner, T.; Wuttig, M.; Zentgraf, T.; Giessen, H. Beam switching and bifocal zoom lensing using active plasmonic metasurfaces. *Light: Sci. Appl.* **2017**, *6*, 17016.

DOI: 10.1021/acsphotonics.8b00699
ACS Photonics 2018, 5, 4056−4060